12 Applications of soft magnets

Don't mention the war.

Temporary magnets concentrate and guide the magnetic flux produced by circulating currents or permanent magnets. Millions of tons of electrical sheet steel are used every year in electromagnetic machinery – transformers, motors and generators. Numerous small components in magnetic circuits are made from nickel–iron alloys, which offer attractive combinations of permeability, polarization and resistivity. Insulating ferrites are particularly suitable for high-frequency applications such as power supplies, chokes and antennae, and for microwave devices.

A good soft magnetic material exhibits minimal hysteresis with low magnetostriction high polarization and the largest possible permeability. Permeability is usually referred to the internal field, because soft magnets tend to be used in a toroidal geometry where demagnetizing effects are negligible. In some range of internal field, the $B(H)$ response is linear $B = \mu H$ or

$$B = \mu_0 \mu_r H, \tag{12.1}$$

where the relative permeability $\mu_r = \mu/\mu_0$ is a pure number. The initial permeability μ_i at the origin of the hysteresis loop is smaller than the slope B/H in slightly larger fields, where it attains its maximum value μ_{max}, as shown in Fig. 12.1. Remanence in a temporary magnet is negligible. The distinction between polarization $J = \mu_0 M$ and induction B is insignificant in applications where device design and high permeability of the soft material ensure that the H-fields involved are very small.

Values of μ_{max}/μ_0 can reach a million in the softest materials. Hence B is hugely enhanced, up to a limit set by the spontaneous induction $B_s \approx J_s = \mu_0 M_s$, compared to the free-space induction $\mu_0 H'$ that induces it. Here H' is the external applied field. Permeability and loop shape can be modified by annealing, especially in a weak external field. The distinction between susceptibility and relative permeability is insignificant when μ_r is very large; it follows from $B = \mu_0(H + M)$ that $\mu_r = 1 + \chi$.

Soft materials may be used for *static* or *AC* applications. The main static and low-frequency AC applications are flux guidance and concentration in magnetic circuits, including cores for transformers and inductors operating at mains frequency (50 or 60 Hz). *Forces* are exerted on current-carrying conductors in motors. Magnetic forces are also exerted between pieces of temporary magnet. Magnetostrictive transducers exert force directly. Changes

Table 12.1. Soft magnetic materials and applications		
Frequency	Materials	Applications
Static <1 Hz	Soft iron, Fe–Co (permendur) Ni–Fe (permalloy)	Electromagnets, relays
Low frequency 1 Hz–1 kHz	Si steel, permalloy, finmet, magnetic glasses	Transformers, motors, generators
Audio-frequency 100 Hz–100 kHz	Permalloy foils, finmet, magnetic glasses, Fe–Si–Al powder (sendust) Mn–Zn ferrite	Inductors, transformers for switched mode power supplies, TV flyback transformers
Radio-frequency 0.1–1000 MHz	Mn–Zn ferrite, Ni–Zn ferrite	Inductors, antenna rods
Microwave >1 GHz	YIG, Li ferrite	Microwave isolators, circulators, phase shifters, filters

Figure 12.1

Hysteresis in a soft magnetic material. $B(H)$ and $J(H)$ are indistinguishable in small fields.
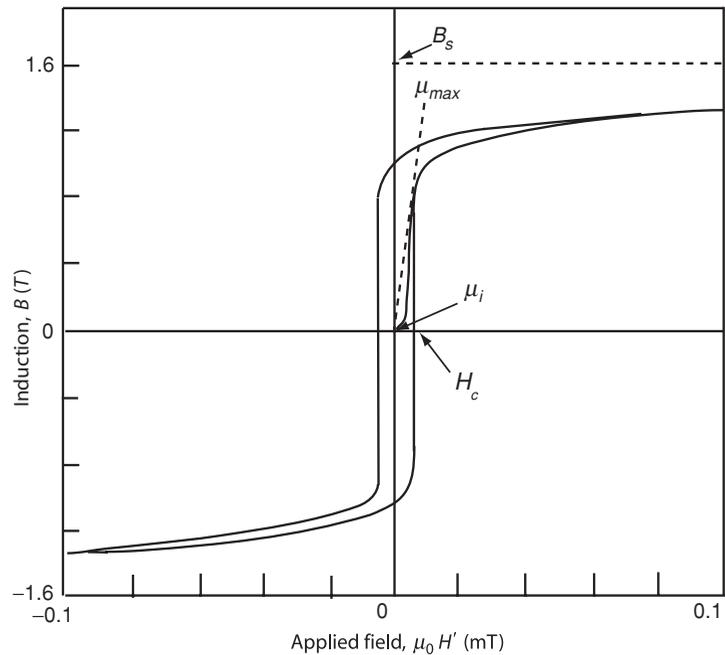
of flux produce *emf* in generators and electronic components. Metals are used up into the kilohertz range, but insulating ferrites are needed to concentrate flux and generate emfs in the radio-frequency and microwave ranges, in order to avoid eddy-current losses. Microwave applications involve the propagation of electromagnetic waves in waveguides rather than currents in electric circuits.

The higher the operating frequency, the lower the permeability and spontaneous induction of the materials used, and the smaller the fraction of saturation at which they operate. Hysteresis increases with frequency, and μ_{max} falls from about 10^4 in electrical steel to 100 or less for ferrites operating in the megahertz range. Preferred materials for the main frequency ranges are specified in Table 12.1.

Figure 12.2

Total loss per cycle showing the three contributions.
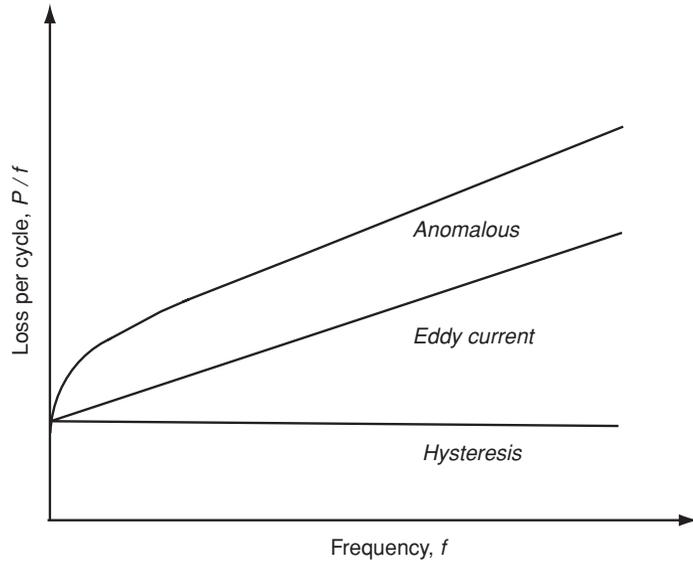
Whenever metals are exposed to an alternating magnetic field, the induced eddy currents limit the depth of penetration of the flux. The skin depth δ_s is defined as the depth where B falls to $1/e$ of its value at the surface:

$$\delta_s = \sqrt{\frac{\varrho}{\pi \mu_r \mu_0 f}}. \tag{12.2}$$

Here ϱ is the resistivity and f is the AC frequency in hertz. For electrical steel ($\varrho = 0.5\,\mu\Omega\,\mathrm{m}$, $\mu_r = 2 \times 10^4$) the value of δ_s is 0.36 mm at 50 Hz. At 500 kHz, it is about 3.6 μm. Cores made from soft magnetic metals are often assembled from a stack of insulated laminations, where the lamination thickness is chosen to be less than δ_s, so that the applied field can penetrate each one. Insulators are untroubled by these problems of flux penetration.
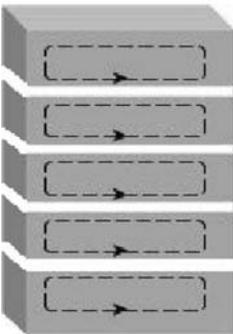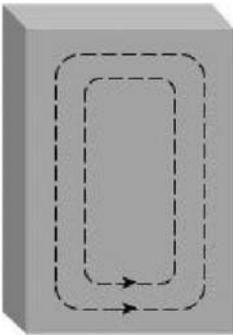
12.1 Losses

12.1.1 Low-frequency losses

Energy losses are critical in any AC application. Traditionally three main sources were identified in soft metallic materials operating at low frequency, as indicated in Fig. 12.2:

- hysteresis loss P_{hy},
- eddy-current loss P_{ed},
- anomalous losses P_{an}.
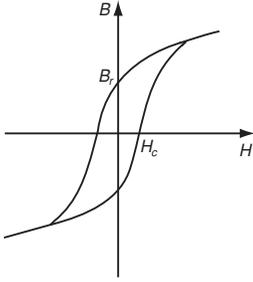
Hysteresis loss per cycle is the area of the $B(H)$ or $\mu_0 M(H')$ loop (Fig. 2.19(c)).

Reduction of eddy-current losses by lamination.

The total losses per cubic metre are therefore

$$P_{tot} = P_{hy} + P_{ed} + P_{an}.$$

Hysteresis loss is related to irreversibility of the static $B(H)$ or $M(H')$ loop. The energy loss per cycle (2.93) is $E_{hy} = \mu_0 \int_{loop} H' \mathrm{d}M$. At a frequency f the loss is $f E_{hy}$

$$P_{hy} = f \mu_0 \int_{loop} H' \mathrm{d}M. \tag{12.3}$$

Eddy-current loss is inevitable when a conducting ferromagnet is subject to an alternating field. The induced currents dissipate their energy as heat. In a sheet of thickness t and resistivity ϱ cycled to a maximum induction B_{max}, the losses P_{ed} vary as f^2:

$$P_{ed} = (\pi \mathrm{t} f B_{max})^2 / 6\varrho. \tag{12.4}$$

These losses can be minimized by using thin laminations or highly resistive material. For example, electrical steel $Fe_{94}Si_6$ (3 wt% Fe–Si) is usually made in laminations about 350 μm thick. It has $\varrho \approx 0.5\ \mu\Omega\,\mathrm{m}$ and density $\mathrm{d} = 7650\ \mathrm{kg\,m^{-3}}$. For $B_{max} = 1\ \mathrm{T}$, it follows from (12.4) that $W_{ed} = P_{ed}/\mathrm{d} \approx 0.1\ \mathrm{W\,kg^{-1}}$ at 50 Hz. Lamination reduces eddy-current losses by a factor $1/n^2$, where n is the number of laminations.

Anomalous losses are whatever remains after P_{hy} and P_{ed} have been taken into account. They turn out to be comparable in magnitude to P_{ed} and they arise from extra eddy-current losses due to domain wall motion, nonuniform magnetization and sample inhomogeneity. Essentially, the anomalous losses reflect the broadening of the hysteresis loop with increasing frequency, so the separation of static hysteresis loss and anomalous loss is artificial. Think of an imaginary circuit containing a moving domain wall; the flux through the circuit is changing, so there is an emf which drives an eddy current near the moving wall.

Anomalous losses are reduced by a structure of many parallel domain walls, which decreases the distance the walls must move during the magnetization process. High-grade electrical steels are therefore laser-scribed to define a structure of narrow stripe domains. Much of the physics in that case is captured by the Pry and Bean model, Fig. 12.3. The electrical sheet is supposed to have a structure of uniformly spaced domains with separation d, which expand and contract in an AC field applied parallel to the walls. The losses in that case are

$$P_{an} = \frac{(4 f B_{max})^2 d \mathrm{t}}{\pi \varrho} \sum_{n\ \mathrm{odd}} \frac{1}{n^3} \coth(n\pi d/\mathrm{t}), \tag{12.5}$$

which reduces to the relation (7.33) in the limit $(d/\mathrm{t}) \gg 1$. Losses for permalloy as a function of frequency are shown in Fig. 12.4.

Figure 12.3

Pry and Bean model for movement of uniformly spaced domain walls. Currents are induced in the neighbourhood of the domain walls, as shown by the dashed lines.
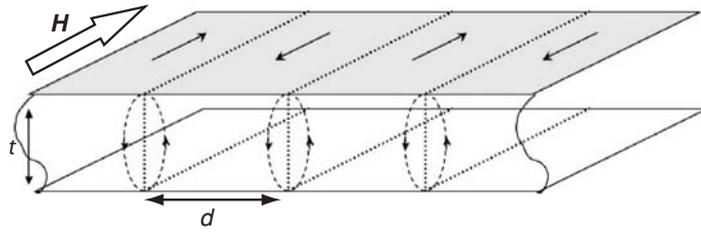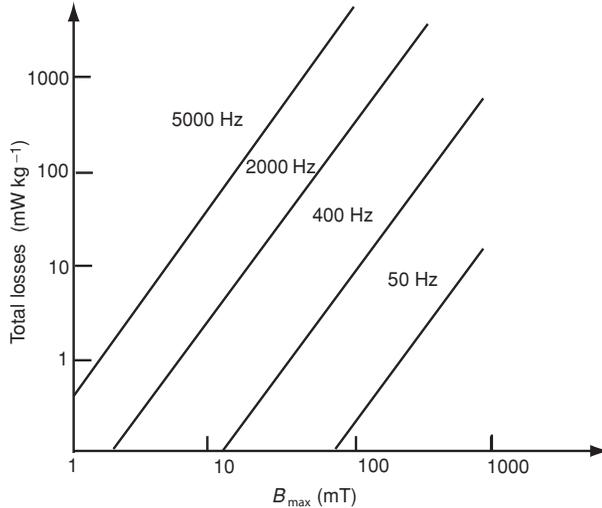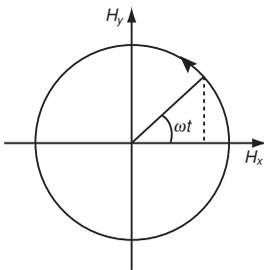

Figure 12.4

Total losses per kilogram for permalloy at different frequencies. Thickness is 350 μm.

A modern physical approach to anomalous losses, due to Bertotti, ascribes the broadening of the hysteresis loop at high sweep rates to the movement of elementary magnetic objects, identified as domain walls or groups of correlated walls. An effective field $H_{an} = P_{an}/(dJ/dt)$ is introduced, where J is the polarization, and the anomalous losses are found to vary as $(fB_{\max})^{2/3}/\varrho^{1/2}$.

Losses in rotating fields are double those in axial fields, because the rotating field can be decomposed into two perpendicular axial components. As the polarization tends to saturation, domain walls are eliminated and the losses tend to zero.

Progress in ameliorating key properties of temporary magnets operating at mains frequencies – core loss and permeability – was dramatic in the twentieth century; they improved by two and four orders of magnitude, respectively, as shown in Fig. 12.5.


A rotating magnetic field $H = H_0 e_x \cos \omega t + H_0 e_y \sin \omega t$.

12.1.2 High-frequency losses

Losses at high frequencies are best represented in terms of a complex permeability. The magnetization process involves magnetization rotation rather than

Progress with soft
magnetic materials during
the twentieth century:
(a) total losses in
transformer cores and
(b) initial static
permeability.
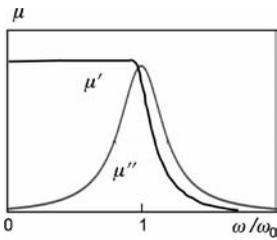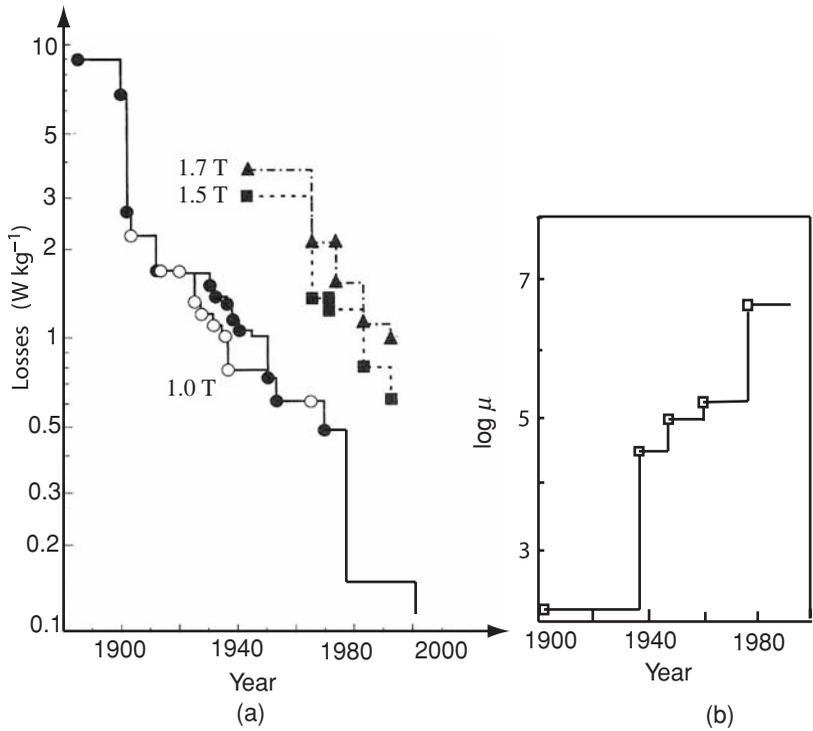
Real and imaginary parts of
the permeability for an
undamped resonance.

domain-wall motion, and losses in the GHz frequency range are influenced by ferromagnetic resonance. If the applied field is $h = h_0 e^{i\omega t}$, the induced flux density $b = b_0 e^{i(\omega t - \delta)}$ generally lags behind by a phase angle δ, known as the loss angle. The real parts of these expressions represent the time-dependent fields $h(t)$ and $b(t)$. The complex permeability $\mu = (b_0/h_0)e^{-i\delta}$ can be expressed as $(b_0/h_0)(\cos\delta - i\sin\delta)$, or

$$\mu = \mu' - i\mu'', \tag{12.6}$$

where $\mu' = (b_0/h_0)\cos\delta$ and $\mu'' = (b_0/h_0)\sin\delta$. The real part of the product μh is the time-dependent flux density

$$b(t) = h_0(\mu' \cos\omega t + \mu'' \sin\omega t), \tag{12.7}$$

so μ' gives the component of b that is in phase with the excitation field h, and μ'' gives the component which lags by $\pi/2$. Losses are proportional to μ'', the response in quadrature with the driving field. The magnetic quality factor Q_m is defined as $(\mu'/\mu'') = \cot\delta$ and the figure of merit is $\mu' Q_m$.

From a knowledge of $\mu'(\omega)$ and $\mu''(\omega)$, the real and imaginary parts of the frequency-dependent permeability of a linear system, it is possible to deduce the response to any small, time-dependent stimulus $h(t)$ which can be expressed

as a Fourier integral

$$h(t) = \frac{2}{\pi} \int_0^\infty h(\omega) \cos \omega t \, \mathrm{d}\omega, \tag{12.8}$$

where the Fourier components are

$$h(\omega) = \frac{2}{\pi} \int_0^\infty h(t) \cos \omega t \, \mathrm{d}t. \tag{12.9}$$

The time-dependent response of the system is the superposition of the responses at different frequencies ω:

$$b(t) = \int_0^\infty [\mu'(\omega) \cos \omega t + \mu''(\omega) \sin \omega t] h(\omega) \mathrm{d}\omega. \tag{12.10}$$

An equivalent expression relates $m(t)$ with $h(\omega)$ in terms of the complex susceptibility $\chi = \chi' - \mathrm{i}\chi''$. Since $\mu_r = 1 + \chi$, it follows that

$$\mu_r' = 1 + \chi' \quad \text{and} \quad \mu_r'' = \chi''.$$

These expressions provide a complete description of the dynamic response of a linear magnetic system. Moreover, the real and imaginary parts of μ or χ are related. Knowledge of one part over the whole frequency range leads to a knowledge of the other, via the powerful Kramers–Kronig relations

$$\mu'(\omega) = \frac{2}{\pi} \int_0^\infty \frac{\mu''(\omega')\omega \mathrm{d}\omega'}{(\omega'^2 - \omega^2)}, \quad \mu''(\omega) = \frac{-2}{\pi} \int_0^\infty \frac{\mu'(\omega')\omega \mathrm{d}\omega'}{(\omega'^2 - \omega^2)}. \tag{12.11}$$

If the sample is anisotropic, the susceptibility and permeability are tensors related by $\hat{\mu} = I + \hat{\chi}$, which can be diagonalized by suitable choice of axes. Each component satisfies the Kramers–Kronig relations.

To calculate the energy losses, we use (2.92) for the work done on a magnetic system. The rate of energy dissipation is $P = h(t)\mathrm{d}b(t)/\mathrm{d}t = h_0^2 \cos \omega t(-\mu'\omega \sin \omega t + \mu''\omega \cos \omega t)$. Since $(1/2\pi) \int_0^{2\pi} \sin \theta \cos \theta \mathrm{d}\theta = 0$ and $(1/2\pi) \int_0^{2\pi} \cos^2 \theta \mathrm{d}\theta = \frac{1}{2}$, the expression for the average rate of energy loss is

$$P_{av} = \tfrac{1}{2}\mu''\omega h_0^2. \tag{12.12}$$

The equivalent expression in terms of the imaginary part of the susceptibility is $\frac{1}{2}\mu_0\chi''\omega h_0^2$. The losses are necessarily positive, which explains the choice of the minus sign in the definition (12.6) of the complex permeability.

To look into the losses associated with the magnetization dynamics in more detail, we consider the damped equation of motion for coherent rotation of the magnetization introduced in Chapter 9:

$$\frac{\mathrm{d}\boldsymbol{M}}{\mathrm{d}t} = \gamma \mu_0 \boldsymbol{M} \times \boldsymbol{H} + \frac{\alpha}{M_s} \boldsymbol{M} \times \frac{\mathrm{d}\boldsymbol{M}}{\mathrm{d}t}, \tag{12.13}$$

where the magnetization vector M has magnitude M_s and it precesses around the direction Oz of the static magnetic field H, which incorporates the applied field, the demagnetizing field and the anisotropy field. The damping term on the right of the Landau–Lifschitz–Gilbert equation causes the magnetization to spiral inwards towards the Oz direction. Damping is essential for any measurement of static magnetization. Without damping, the spontaneous magnetization would precess perpetually around the applied field and never align with it.

We consider the case where a field is applied along an easy anisotropy axis. The equilibrium value of M is M_s, aligned along Oz. The instantaneous value of M is inclined at an angle θ and the deviation m is defined as $M - M_s$. The effective field H_s, also along Oz, is the sum of the applied field H and the effective anisotropy field $H_a \cos \theta$. The torque is $\boldsymbol{\Gamma} = \gamma \mu_0 M \times H_s$. Next we apply an alternating magnetic field $h = h_0 \cos \omega t$ in the xy-plane. In the undamped case,

$$\mathrm{d}M/\mathrm{d}t = \gamma \mu_0 M \times (H_s + h). \tag{12.14}$$

The equation is linear when the perturbation is small, that is when $h \ll H_s$ and $m \ll M_s$, Thus

$$\mathrm{d}M/\mathrm{d}t = \gamma \mu_0 (m \times H_s + M_s \times h). \tag{12.15}$$

In component form

$$\frac{\mathrm{d}m_x}{\mathrm{d}t} - \gamma \mu_0 H_s m_y = \gamma \mu_0 M_s h_y, \tag{12.16}$$

$$\frac{\mathrm{d}m_y}{\mathrm{d}t} + \gamma \mu_0 H_s m_x = -\gamma \mu_0 M_s h_x, \tag{12.17}$$

$$\frac{\mathrm{d}m_z}{\mathrm{d}t} = 0. \tag{12.18}$$

In complex notation $\mathrm{d}/\mathrm{d}t$ is replaced by $i\omega$. Setting $\omega_0 = \gamma \mu_0 H_s$ and $\omega_M = \gamma \mu_0 M_s$, the equations are written

$$\begin{bmatrix} \omega_0 & i\omega & 0 \\ i\omega & -\omega_0 & 0 \\ 0 & 0 & 0 \end{bmatrix} \begin{bmatrix} m_x \\ m_y \\ m_z \end{bmatrix} = \omega_M \begin{bmatrix} -h_x \\ h_y \\ h_z \end{bmatrix},$$
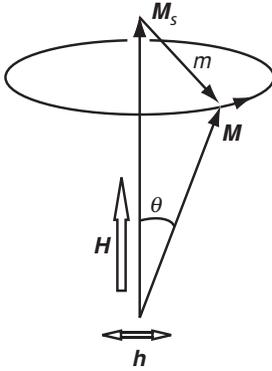
which can be inverted to read

$$\begin{bmatrix} m_x \\ m_y \\ m_z \end{bmatrix} = \begin{vmatrix} \kappa & -i\nu & 0 \\ i\nu & \kappa & 0 \\ 0 & 0 & 0 \end{vmatrix} \begin{bmatrix} h_x \\ h_y \\ h_z \end{bmatrix},$$

where

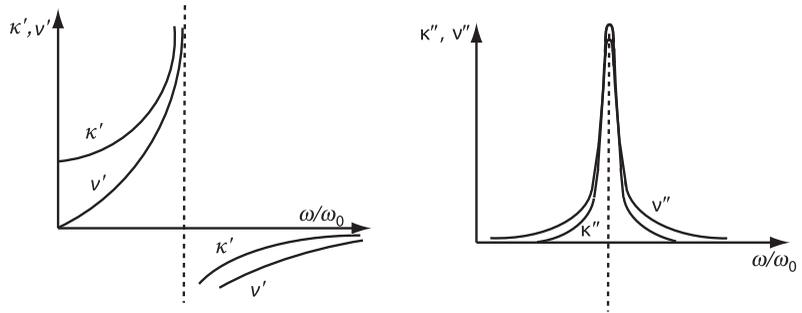$$\kappa = \omega_0 \omega_M / (\omega_0^2 - \omega^2) \tag{12.19}$$

and

$$\nu = \omega \omega_M / (\omega_0^2 - \omega^2). \tag{12.20}$$

Magnetization precession.

Figure 12.6

Real and imaginary parts of
the susceptibilities κ and ν.

This susceptibility tensor describes the precession of the magnetization for uniaxial anisotropy in the absence of damping. Only the in-plane components need be considered, so

$$|\chi| = \begin{bmatrix} \kappa & -i\nu \\ i\nu & \kappa \end{bmatrix}.$$

When $\omega = 0$, $\nu = 0$, the tensor reduces to a scalar: $\chi_0 = \omega_M/\omega_0 = M_s/H_s$. As $\omega \longrightarrow \omega_0$, the ferromagnetic resonance frequency, κ, and ν diverge as shown in Fig. 12.6. The product of the static susceptibility and the resonance frequency $\chi_0\omega_0 = \omega_M$ is constant:

$$\chi_0\omega_0 = \gamma\mu_0 M_s. \tag{12.21}$$

This is Snoek's relation. The greater is the ferromagnetic resonance frequency ω_0, the lower is the static susceptibility χ_0. Unfortunately, extending the frequency response of ferrites leads to a decline in susceptibility and loss of performance.

In the case of a polycrystalline sample of volume v having crystallites of volume v_i with randomly oriented easy axes, the induced magnetization $\mathfrak{m} = \sum_i v_i \chi h = \chi_{eff} h$. The susceptibility $\chi_{eff} = \frac{2}{3}\kappa = 2\omega_M\omega_0/3(\omega_0^2 - \omega^2)$. The product of the static susceptibility and the resonance frequency in this case is $\chi_0\omega_0 = \frac{2}{3}\omega_M = \frac{2}{3}\gamma\mu_0 M_s$. This shows that it is impossible to exceed the Snoek limit in such a system, but it can be circumvented in ferrites with strong planar anisotropy. Ferrites are used as phase shifters in microwave applications above 10 GHz.
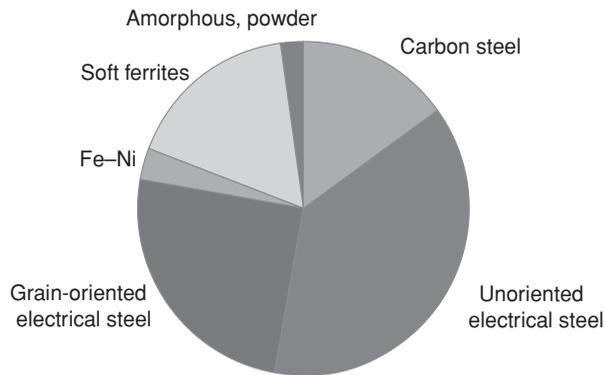
When damping is taken into consideration, a term $-(\alpha/M_s)\mathbf{M} \times d\mathbf{m}/dt$ is added to (12.15). The new expressions for κ and ν are

$$\kappa = \frac{\omega_M(\omega_0 + i\alpha\omega)}{\omega_0^2 - (1 + \alpha^2)\omega^2 + i2\alpha\omega\omega_0}, \tag{12.22}$$

$$\nu = \frac{\omega_M\omega}{\omega_0^2 - (1 + \alpha^2)\omega^2 - i2\alpha\omega\omega_0}. \tag{12.23}$$

Figure 12.7

Global market for soft magnetic materials. The pie represents about 10 B$ per year.

12.2 Soft magnetic materials

The global market for soft magnetic materials is summarized in Fig. 12.7. Electrical steel for transformers and electromagnetic machinery is predominant. Produced in quantities in excess of 7 million tonnes per year, it represents about 1% of global steel production, but 95% of the tonnage and 75% of the market value of all temporary magnets. The choice of soft magnetic material is a trade-off between polarization, permeability, losses and cost. The polarization should be as large as possible for a given excitation field, and core losses must be acceptable at the operating frequency. Alloy additions such as C, Si or Al, which reduce losses and increase permeability also reduce the saturation polarization and increase cost. One alloy does not suit all needs, but there are a few widely used grades, which have been optimized over the years.

Low-carbon mild steel is used for cheap motors in consumer products such as washing machines, vacuum cleaners, refrigerators and fans, where losses are of little interest to the manufacturer. The customer pays for the electricity. Better electrical performance requires other alloy additions. Silicon is ideal, because 4 at% suffices to suppress the $\alpha \rightarrow \gamma$ phase transition in iron, permitting hot rolling of the sheet. Traces of carbon extend the γ phase stability region, so the silicon content is usually around 6 at% or 3 wt%. Silicon steel was invented by Robert Hadfield in 1900, who found that the 6 at% Si composition was sufficiently ductile to be rolled into thin sheets. Isotropic and grain-oriented $Fe_{94}Si_6$ in the form of sheets about 350 μm thick is produced by the square kilometre for mains-frequency electrical applications. Losses are about ten times lower than for mild steel. Silicon increases the resistivity, and reduces both the anisotropy and the magnetostriction of the iron. *Isotropic* sheet is appropriate for motors and generators, where the direction of flux changes continually during operation. In transformers, however, the axis of B is fixed, and it is beneficial to use *crystallographically oriented* sheet with an easy axis to further reduce losses. This material was developed by the felicitously named
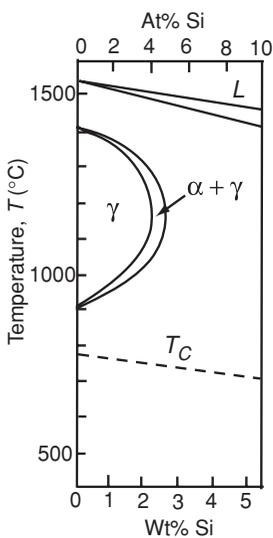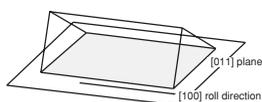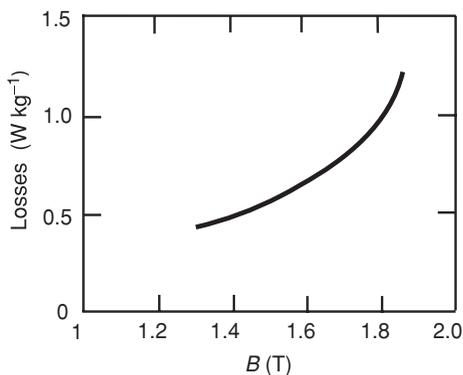

Iron-rich side of the Si–Fe phase diagram.

Table 12.2. Properties of magnetic sheet steels					
Material	J_s (T)	μ_r at 1.5 T	H_c (A m^{-1})	W_{tot} (W kg^{-1})	ϱ ($\mu\Omega$ m)
Mild steel	2.15	500	80	12	0.15
Si steel	2.12	1 000	40	2.5	0.60
Grain-oriented Si steel	2.00	20 000	5	1.2	0.50

Figure 12.8

Losses as a function of operating induction for grain-oriented silicon steel.

The Goss texture of grain-oriented Si–Fe.

Norman Goss in 1934. It went into mass production in 1945, and now accounts for around 20% of the volume of electrical steel produced. *G*rain-*o*riented *s*ilicon *s*teel with the Goss texture is produced by an extended process of rolling and annealing which promotes secondary crystallization. The {110} planes of the secondary crystallites are parallel to the sheets and a [100] easy axis is parallel to the roll direction. The losses at 1.7 T are below 1 W kg^{-1}, but they increase as the material operates closer to saturation, Fig. 12.8.

The thickness of grain-oriented silicon steel laminations is 200–350 μm. Thinner Si–Fe sheet can be produced by planar flow casting. The thinner laminations are useful at higher frequencies, and for reducing losses for non-sinusoidal waveforms with a high harmonic content, which arise, for example, from wind farms. The properties of different magnetic steels are compared in Table 12.2.

A great range of useful magnetic properties can be achieved in the Ni–Fe alloy system. Here the economic benefit is measured not so much in thousands of tonnes as in millions of magnetic components of widely differing shapes and sizes. The outstanding feature of Ni–Fe alloys is their permeability, which is achieved by carefully controlled heat treatment. Interesting compositions, between 30% and 80% nickel, have the fcc γ Ni–Fe structure. A weak uniaxial anisotropy of order 100 Jm^{-3} can be induced in Ni–Fe alloys by magnetic field annealing to help control the magnetization process. Most remarkable are the permalloys with composition close to Ni$_{80}$Fe$_{20}$, where both anisotropy and magnetostriction fall to zero at almost the same composition. This promotes the

Table 12.3. Properties of soft materials for static or low-frequency applications

Material	Name	μ_i	μ_{max}	J_s (T)	H_c (A m^{-1}))
Fe	Soft iron	300	5 000	2.15	70
$Fe_{49}Co_{49}V_2$	V-permendur	1 000	20 000	2.40	40
$Ni_{50}Fe_{50}$	Hypernik	6 000	40 000	1.60	8
$Ni_{77}Fe_{16.5}Cu_5Cr_{1.5}$	Mumetal	20 000	100 000	0.65	4
$Ni_{80}Fe_{15}Mo_5$	Supermalloy	100 000	300 000	0.80	0.5
a-$Fe_{40}Ni_{38}Mo_4B_{18}$	Metglas 2628SC	50 000	400 000	0.88	0.5
$Fe_{73.5}Cu_1Nb_3Si_{13.5}B_9$	Finmet	50 000	800 000	1.25	0.5

highest, shock-insensitive permeability. A tendency towards Ni_3Fe-type $L1_2$ atomic ordering can be suppressed by Mo additions in supermalloy, and ductility is achieved with copper additions in mumetal, which is good for magnetic shielding. Larger polarization is obtained near the equiatomic $Ni_{50}Fe_{50}$ composition (hypernik), but the soft magnetic properties are slightly inferior to those of permalloy (Table 12.3). The iron-rich invar alloys, around $Ni_{36}Fe_{64}$, offer low Curie temperatures and rapid thermal variation of the spontaneous polarization, which are exploited in applications such as rice cookers and electricity meters. Their dimensional stability around room temperature due to negative volume magnetostriction makes them suitable for mechanical precision instruments. Charles Guillaume received the Nobel prize in 1920 for his discovery of invar, the only time the prize was awarded for a new magnetic material.

The Co–Fe alloys are much less versatile, and more expensive. The cost of cobalt used to fluctuate wildly, but it stabilized as more geographically diverse sources of supply became available. The great advantage of permendur, $Fe_{50}Co_{50}$, is its polarization, the highest of any bulk material at room temperature (2.45 T). Addition of 2% vanadium improves the machinability without spoiling the magnetic properties. The $Fe_{65}Co_{35}$ composition provides similar polarization with less cobalt.

Powder of iron or the brittle zero-anisotropy, zero-magnetostriction alloy *Sendust* ($Fe_{85}Si_{10}Al_5$) can be insulated and used at higher frequencies in cores. Iron powder with a particle size of a few micrometres is practically anhysteretic at all temperatures (Fig. 12.9). Relative permeability is limited to 10–100 because of the demagnetizing fields. Long telephone lines are loaded with powder-core inductors (loading coils) to balance their capacitance.

Melt-spun amorphous alloy ribbons can be produced with thickness of about 50 μm and resistivity $\approx 1.5\,\mu\Omega$ m. No higher resistivity can be achieved in a metal because it corresponds to a mean-free path comparable to the interatomic spacing. The compositions are close to the glass-forming ratio $M_{80}T_{20}$, where T = Fe, Co, Ni and M = B, Si. Cobalt-rich compositions exhibit zero magnetostriction, and permeability up to 10^6. Metallic glass ribbons can be wound into cores for use up to about 100 kHz, and applied, for example, in

Magnetization of diluted
iron powder with a particle
size of 6–8 µm. (Data
courtesy of M. Venkatesan.)

An assortment of
soft-magnetic components
made from finmet.
(Courtesy, Hitachi metals.)
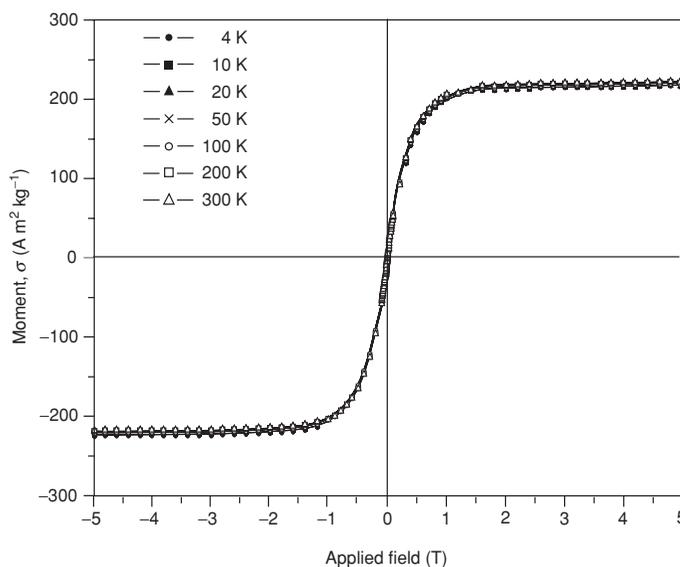
switched mode power supplies, distribution transformers, as well as in flux gate
magnetometer. Partially crystallized nanocrystalline materials such as finmet
(§11.2.4) offer comparable permeability, with higher polarization.

Soft ferrites have mediocre polarization and permeability compared to
metallic ferromagnets – their ferrimagnetic saturation polarization is only
0.2–0.5 T – but their insulating character is a decisive advantage at high fre-
quencies. Since eddy-current losses are not a problem, there is no need for
lamination. Oxides are also much better than metals at resisting corrosion.
Ceramic components have to be produced to near-net shape, and finished by
grinding.

Magnetic properties of the spinel ferrites have been tailored by tuning the
composition, microstructure and porosity since the 1940s when these materials
first saw the light of day in the Netherlands. Mn–Zn ferrites are used up
to about 1 MHz, and Ni–Zn ferrites from 1–300 MHz or more. The latter
have lower polarization, but higher resistivity. Conduction is usually due to
traces of Fe^{2+}, which promotes Fe^{2+}–Fe^{3+} electron hopping. Most cations
make a negative contribution to the magnetostriction and anisotropy constant;
$\langle 111 \rangle$ directions in the spinel lattice are usually easy, unless Co^{2+} or Fe^{2+} are
present.

The frequency response of the initial permeability of a ferrite μ_i is almost
flat up to a rolloff frequency f_0, associated with ferromagnetic resonance
(Fig. 12.10). The losses peak at f_0. The permeability and resonance frequency
vary oppositely with anisotropy, and according to Snoek's relation (12.21) their
product is constant for a particular compositional family: the higher the rolloff
frequency, the lower the permeability. The figure of merit $\mu_i f_0$ is about 8 MHz

Table 12.4. Properties of soft materials for high-frequency applications

Material	J_s(T)	μ_i	H_c (A m^{-1})	ϱ (Ω m)	P (0.2T)
Mn–Zn ferrite	0.45	4000	20	1	200
Ni–Zn ferrite	0.30	500	300	$>10^3$	

Figure 12.10

Frequency response of the real and imaginary parts of the permeability for some Ni–Zn ferrites with different permeability. (After Smit and Wijn (1979).)
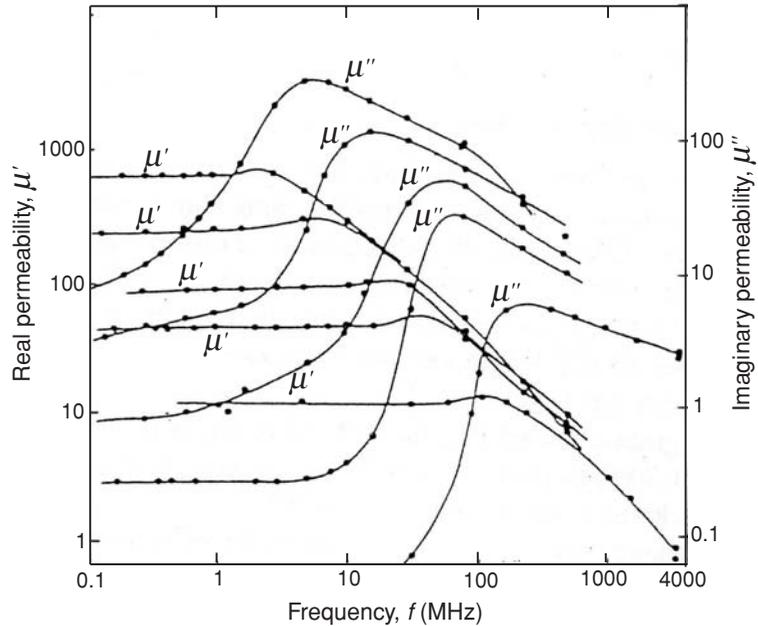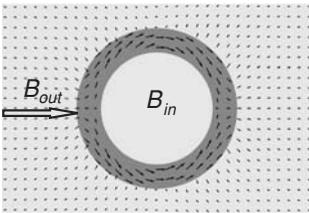

for Ni–Zn ferrites and 4 GHz for MnZn ferrites. Hence it is not feasible for a MnZn ferrite with a permeability of 10 000 to operate above 400 kHz. Properties of high-frequency ferrites are summarized in Table 12.4.

YIG is an excellent microwave material for use in the GHz range. Highly perfect insulating crystals can be prepared which have minimal anisotropy. To measure the ferromagnetic resonance, a small sample ground and polished in the form of a sphere is placed near the end of a waveguide. The reflected signal is measured at fixed frequency as the applied field is swept through the resonance at $\omega_0 = \gamma H_0$, where γ is the gyromagnetic ratio ≈ 28 GHz T^{-1}. In the X-band (8–12 GHz radiation, handled in 25 mm waveguides) the linewidth of the resonance observed in an applied field of 350 kA m^{-1}, may be only 350 A m^{-1} for dense polycrystalline YIG and better than 35 A m^{-1} for a single-crystal sphere. The Q factor $\omega/\Delta\omega$ is therefore 1000 in one case and 10 000 in the other. These sharp resonances are indispensable for microwave filters and oscillators. The snag is that a magnetic field is needed to operate these components, which must be provided by an electromagnet or a permanent magnet.

12.3 Static applications

An electromagnet.

Magnetic shielding. The shielding ratio $\mathcal{R}$ is B_{out}/B_{in}.

Electromagnets consist of field coils to polarize an iron core, a yoke to guide the flux and pole pieces to concentrate flux in the airgap, Fig. 12.11. Flux guidance and concentration in electromagnets requires material with the highest polarization and very little remanence. Pure soft iron or $Fe_{65}Co_{35}$ is used. For best results, the pole pieces are tapered at an angle of $55°$.

Electromagnetic relays and solenoid valves are miniature electromagnets where an iron core is magnetized and exerts a force on another temporary magnet. When the gap flux density is B_g, the force per unit area is $B_g^2/2\mu_0$ (13.13).

Passive magnetic shielding of low-frequency AC fields or weak DC fields, such as the Earth's, requires material to provide a low-reluctance flux path around the shielded volume. Reluctance is the magnetic analogue of resistance. The shielding ratio $\mathcal{R}$ is the ratio of the field outside to the field inside. Values of $\mathcal{R} \approx 100$ are achieved in low fields. The thickness of shielding material is chosen so that its polarization is unsaturated by the flux collected. It is more effective to use several thin shields rather than one thick one. DC shields are often made of permalloy or mumetal, which have negligible anisotropy and magnetostriction, and are therefore immune to shock and strain. Flexible shielding woven from cobalt-rich metallic glass tape, or finmet sheet may be used directly.

12.4 Low-frequency applications

Figure 12.12

Types of cores: (a) stacked laminations, (b) tape-wound core, (c) powder core (sectioned to show internal structure) and (d) ferrite E-core.

(a)   (b)

(c)   (d)
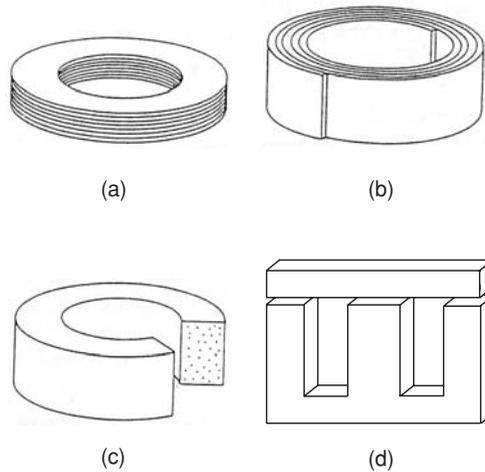
Inductors are one of the three basic components of electric circuits. They are circuit elements that resist any change of current through them. The voltage drop across a resistanceless inductance of L henry is $V(t) = -L\partial I/\partial t$. If $I = I_0 \sin \omega t$, the resulting voltage $LI_0\omega \cos \omega t$ has a phase lag of exactly $\pi/2$. Consider the inductor as a long solenoid with cross section $\mathcal{A}$, length l and n turns per metre. The flux density in the solenoid is $\mu_0 n I$. By Faraday's law $V = -\partial \Phi/\partial t = -\mu_0 n^2 l \mathcal{A} \partial I/\partial t$; hence $L = \mu_0 n^2 l \mathcal{A}$. Filling the solenoid with soft magnetic material of permeability μ_r increases the flux density by this factor, so that

$$L = \mu_0 \mu_r n^2 l \mathcal{A}. \tag{12.24}$$

An inductor with and without a soft magnetic core.

The soft magnetic core therefore increases the electrical inertia of the inductor by orders of magnitude. Alternatively, the dimensions of a component with a given inductance can be greatly reduced by including a soft core. Some commonly used ones are shown in Fig. 12.12.

Low-frequency electrical machines include transformers, motors and generators that operate at mains frequencies of 50 or 60 Hz, or 400 Hz in the case of airborne or shipborne power. They include soft iron cores to generate and guide the flux. Eddy-current losses (12.4) are reduced by using thin laminations of material with a high resistivity. Efficiencies of well-designed transformers exceed 99%; they are probably the most efficient energy converters ever made. Core losses represent about a quarter of the total, the remainder being in the windings. The core losses in transformers nevertheless cost some 10 billion dollars per year. World-wide annual consumption of electrical energy is around 18×10^{12} kW h, which corresponds to an average rate of consumption of

Figure 12.13

Two electric motor designs:
(a) an induction motor and
the squirrel cage (b) a 3/4
variable reluctance motors.
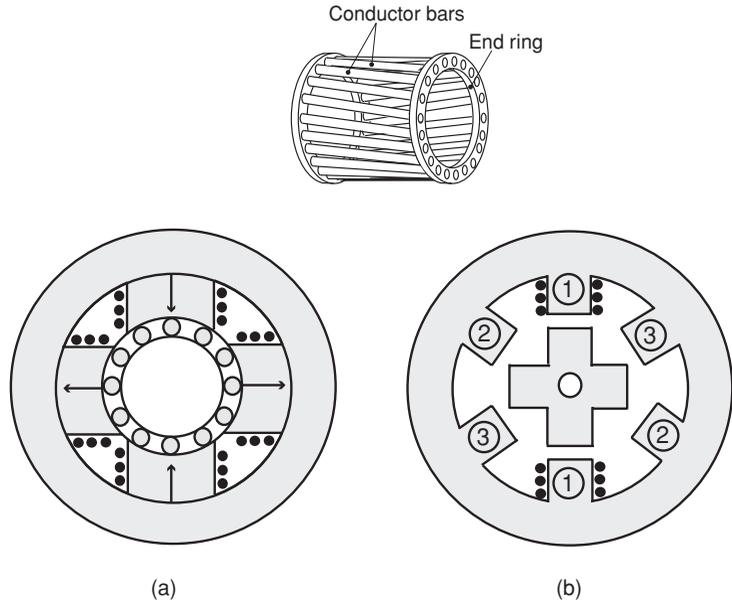
300 W per head of population. The rich billion of the Earth's people consume about ten times as much, and the poorest billion almost none at all.

Electricity is produced in power stations by large turbogenerators (~1000 MW) turning at constant frequency. The mains power is generated at a multiple of this frequency so it is unnecessary to use laminations in the rotor.

Electric motors are manufactured by the million. Whether they are excited by field coils or permanent magnets, they incorporate quantities of temporary magnets to guide the flux. Here we will describe just two designs which consume much electrical steel. The induction motor is the simplest and most rugged of all (Fig. 12.13(a)). It is manufactured in sizes ranging from 10 W to 10 MW for a myriad of domestic and industrial applications. The 'fractional horse power'[1] motors in consumer goods are usually induction motors.

The stator of this workhorse is a hollow cylindrical stack of laminations, pressed into a core, with slots to receive the field windings. The windings are energized with single-phase mains power (three-phase for industrial drives), which creates a rotating magnetic field in the centre. There is a 'squirrel cage' rotor consisting of metal bars running parallel to the axle which are short-circuited by circular end rings, and another soft-iron core is mounted in the centre. The forces on currents induced in the squirrel cage cause it to rotate with the field, but at slightly less than synchronous speed. It is an *asynchronous* motor which draws maximum current at startup.

---

[1] 1 horse power = 746 W.

(a) Schematic diagram of a fluxgate magetometer, (b) principle of operation. The cores are saturated in the sum of the AC field h and the applied field H'. The pickup voltage V is proportional to H'.

(a)   (b)
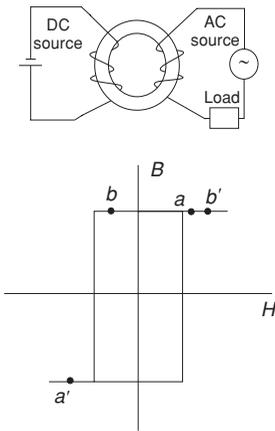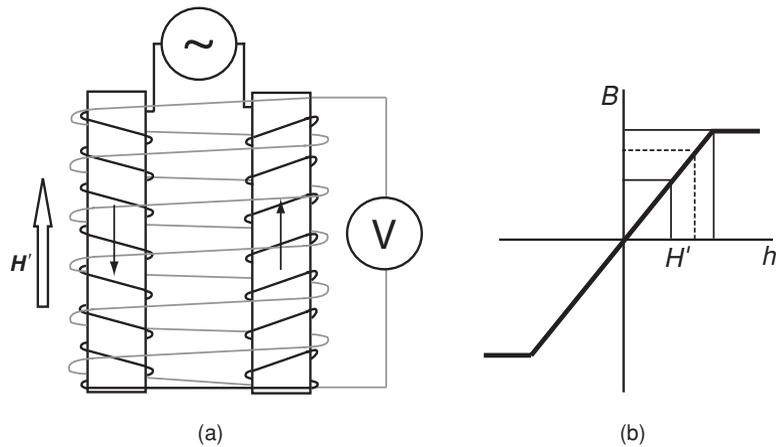
A magnetic amplifier. With no DC control current, there is a large flux swing (a–a'), but as the control current rises the flux swing ceases (b–b'') and the AC load current rises.

A different operating principle applies in the variable-reluctance motor. Reluctance is the magnetic resistance associated with the flux path. The analogy between electric and magnetic circuits is developed in §13.1. A 3/4 motor design is illustrated in Fig. 12.13(b). There are three pairs of stator windings, which are energized in the sequence 1–2–3 to create a rotating field. The rotor this time is just a piece of laminated soft iron with four poles in the form of a cross. Initially it is in the position shown, but when windings 2 are energized, it rotates clockwise by $60°$, and so on. The motor is synchronous. It offers a high torque to inertia ratio, but it requires a precise electronic controller to power the windings.

Magnetic amplifiers use square-loop cores which may be made from textured $Ni_{50}Fe_{50}$. When the DC control current is zero, the load current passing through the AC winding is very small because the voltage drop across the winding, proportional to $d\Phi/dt$, almost cancels the source signal. As the current from the DC source saturates the core, the change in flux in the core becomes negligible and the current in the load rises.

A related application which depends on saturable soft cores is the fluxgate magnetometer, Fig. 12.14. The magnetometer consists of two identical, parallel cores with a field winding creating an AC field, h, in opposite directions. A toroidal core with a helical winding will work as well. The field, H', to be measured is applied parallel to the cores, and it leads to periodic saturation of one of them. The changing flux is sensed in a secondary coil usually with the help of a lockin detector. A response linear in applied field is obtained by flux compensation to null the signal. Fields of up to $200 \, \text{A m}^{-1}$ can be measured with an accuracy of $0.5 \, \text{A m}^{-1}$. Typical noise figures are $100 \, \text{pT Hz}^{-1/2}$.

A different family of applications of soft magnets makes use of their magnetostrictive properties, which generally depend on the direction of magnetization relative to the crystal axes. The linear saturation magnetostriction λ'_s of an isotropic polycrystalline material is an average over all directions. Nickel, for example, has $\lambda_s = -36 \times 10^{-6}$, so modest strains can be achieved

Figure 12.15

A surface acoustic wave
delay line.
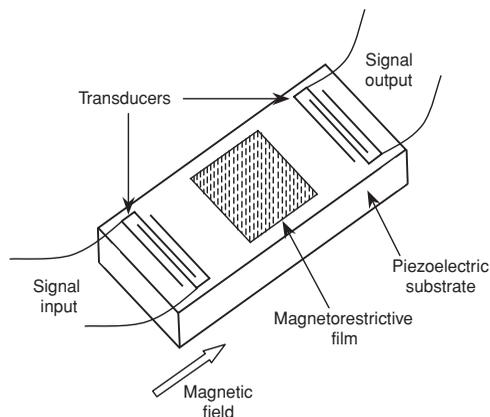
by magnetizing nickel rods. Grain-oriented silicon steel has $\lambda_{100} = 20 \times 10^{-6}$,
which is why transformers hum. Much larger effects are obtained with the
mixed Tb–Dy alloy terfenol (§11.3.5), where cancellation of cubic anisotropy
contributions of opposite sign for the two rare-earths means the alloy is easy to
magnetize. The huge linear magnetostriction of 1500×10^{-6} makes it useful
for linear actuators and ultrasonic or accoustic transducers, including sonar.

Another manifestation of magnetostriction in a soft magnetic material is
the ΔE effect (§5.6.2). The dramatic softening of Young's modulus, as the
domains align in a small field, can be used to tune a surface accoustic wave
delay line, Fig. 12.15, of the type incorporated in military radar. The accousic
wave propagates in a piezzoelectric substrate such a quartz or LiMbO$_3$, where
it is excited and detected by a pair of interdigitated transducers. The beam from
an array of antennae can be directed by tuning the time delays between adjacent
elements of the array.

12.5 High-frequency applications

Ferrite components are extensively employed in high-frequency applications,
although metallic alloys with very thin laminations offer the benefit of higher
polarization at frequencies where the losses are not too severe.

Ferrite cores appear in chokes, inductors and high-frequency transformers
for switched-mode power supplies. They are also used for broad-band ampli-
fiers and pulse transformers. Losses at 100 kHz are about 50 W kg^{-1}. Another
common application of ferrites is as antenna rods in AM radios, Fig. 12.16.
The ferrite antenna consists of an N-turn pickup coil wound on a rod of cross-
sectional area $\mathcal{A}$. The voltage induced by a radio-frequency field of amplitude
b_0 and frequency ω would have amplitude $N\omega\mathcal{A}b_0$ for the coil alone. The

Figure 12.16

(a) A wire loop antenna, and (b) an equivalent ferrite rod with much smaller cross section.

(a)   (b)
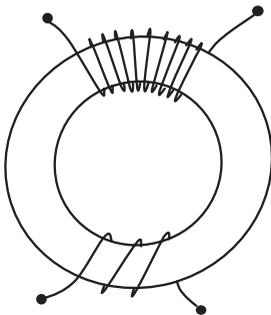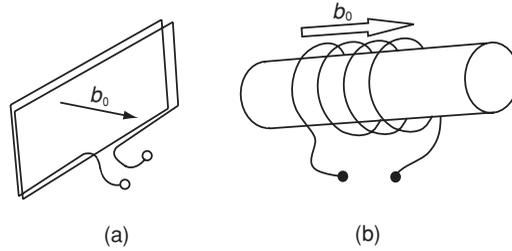
A pulse transformer.
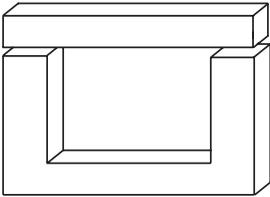
AC core with an airgap.

external susceptibility of a piece of soft material with demagnetizing factor $\mathcal{N}$ was given by (2.42) $\chi'_e = \chi(1 + \chi\mathcal{N})'$.

In the present case, $\mathcal{N}$ is small and μ is very large, so that $\chi = \mu$, and $\chi\mathcal{N} \gg 1$. Hence $\mu' \sim 1/\mathcal{N}$. The amplitude of the voltage induced in the antenna is therefore $N\omega A b_0/\mathcal{N}$. The ferrite acts as a flux concentrator, so that the antenna is equivalent to a much larger bare coil of area $\mathcal{A}/\mathcal{N}$. Ni–Zn ferrite is best for this application on account of its high resistivity.

The wide frequency range over which ferrites exhibit near constant μ' and negligible μ'' (Fig. 12.10) makes them suitable for pulse transformers. A pulse that is sharply defined in time contains Fourier components spanning a wide range of frequencies. The transformer is just a ring of soft ferrite on which both the primary and secondary are wound.

A single grade of ferrite can be used to produce high-frequency inductors of a standard size with different values of L by the expedient of leaving an airgap in the core. If l_m is the length of the core which has permeability μ, l_g is the length of the airgap and $\mathcal{A}$ is the cross section, the reluctance is the sum of the contributions of the ferrite and the airgap (13.5), which can be written as $(l_m/\mu_0\mu_{eff}\mathcal{A}) = (l_m/\mu_0\mu_r\mathcal{A}) + (l_g/\mu_0\mathcal{A})$. Hence

$$\frac{1}{\mu_{eff}} \approx \frac{1}{\mu_r} + \frac{l_g}{l_m} \approx \frac{l_g}{l_m}. \tag{12.25}$$

The cross section can be obtained when the permeability is degraded by the airgap, which introduces a demagnetizing field in the ferrite. The effective demagnetizing factor of the gapped core is $\mathcal{N} = l_g/l_m$.

Miniature inductors can be integrated with on-chip electronics. A planar or bilevel copper coil and a thin permalloy core can be electroplated and sputtered directly onto the chip.

Resonant filters are LC circuits which pass a narrow band of frequencies, whose width is limited by losses in the components, Fig. 12.17. The relative width of the peak gauged at the point where the value falls to $1/\sqrt{2}$ of the peak value is[2]

$$\frac{\Delta\omega}{\omega_0} = \frac{1}{Q}, \tag{12.26}$$

[2] The external susceptibility χ' in the applied field H' should not be confused with the real part of the complex susceptibility, which also features in this chapter.

Figure 12.17

An LC filter circuit and the pass band.
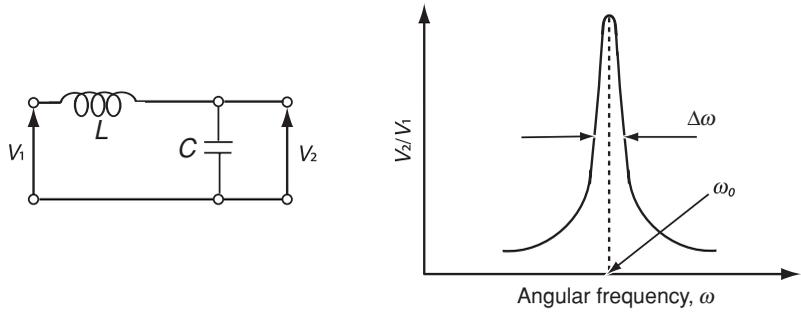
where the Q factor is essentially limited by resistive losses in the inductor. Q is defined as μ'/μ''. The quality factor is maximized when the losses are equally divided between the copper windings and the magnetic material; Q is then $L\omega/2R$.

12.5.1 Microwave applications

Microwave ferrites can operate in the frequency range 300 MHz–100 GHz. At these frequencies, we need to consider the electromagnetic wave travelling in a waveguide rather than the current in a circuit. Microwave devices exploit the nonreciprocal interaction of the electromagnetic field with the ferromagnetic medium, especially in the vicinity of the ferromagnetic resonance frequency ω_0. Generally, if a uniform external field is applied along Oz and an AC field h' is applied in the xy-plane, the resulting flux density B is given by the tensor permeability

$$\begin{bmatrix} B_x \\ B_y \\ B_z \end{bmatrix} = \begin{bmatrix} \mu' & -i\mu'' & 0 \\ i\mu'' & \mu' & 0 \\ 0 & 0 & \mu_0 \end{bmatrix} \begin{bmatrix} H'_x \\ H'_y \\ H'_z \end{bmatrix}, \tag{12.27}$$

where $H' = H_z + h$. The off-diagonal terms produce the nonreciprocal effects.

A plane-polarized wave $h = h_0 \cos \omega t$ can be decomposed into two oppositely rotating circularly polarized waves.

$$h = h_0 \cos \omega t = \frac{h_0}{2}(e^{i\omega t} + e^{-i\omega t}), \tag{12.28}$$

which generally propagate at different speeds $c/\sqrt{\epsilon\mu_+}$ and $c/\sqrt{\epsilon\mu_-}$. This magnetic circular birefringence is the microwave Faraday effect. The $+$ and $-$ directions are defined in relation to the polarization of the ferrite. Here μ_+ and μ_-, the effective permeabilities for right and left polarizations, are $\mu_+ = \mu'_+ - i\mu''_-$ and $\mu_- = \mu'_- + i\mu''_-$, Fig. 12.18. The first turns in the sense of the Larmor precession and shows a resonance at the ferromagnetic resonance frequency, the second turns in the opposite sense and does not resonate. If the plane wave is incident normal to the surface of a plaque of ferrite of
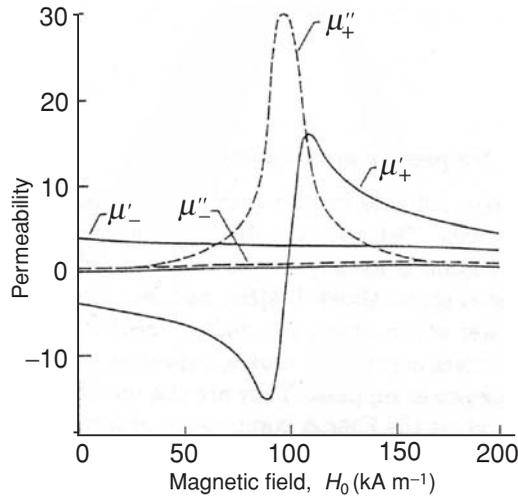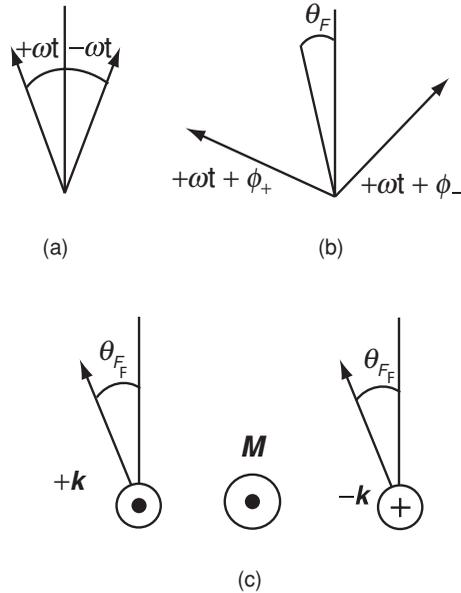
Absorption and
transmission for left- and
right-polarized radiation.

Two counter-rotating
circularly polarized waves
(a), which become
dephased because they
propagate with different
velocities (b), producing
the Faraday roation θ_F (c).
The effect does not depend
on the sense of
propagation of the waves
relative to the
magnetization of the
birefringent medium.

thickness t, the two counter-rotating modes become dephased by an angle
$\phi_{\pm} = \sqrt{(\epsilon\mu_{\pm})}\omega t/c$, and the plane of polarization is rotated through an angle
$\theta = (\phi_{+} + \phi_{-})/2$ when it traverses the ferrite, as shown in Fig. 12.19. This is
the microwave Faraday effect. Unlike the Faraday effect at optical frequencies,
where $\mu = \mu_0$, which is of order 10^{-4} radians for $d = \Lambda$, the rotation at
microwave frequencies is of order 1 radian per wavelength, so it is best to place
ferrite components inside the waveguides.

The Faraday effect is nonreciprocal in the sense that the direction of rotation
of the plane of polarization of the light does not depend on the direction of

A waveguide propagating a
TE_{01} mode. Filling the upper
half with YIG magnetized
vertically absorbs the
microwaves for one
direction of propagation,
but not the other.
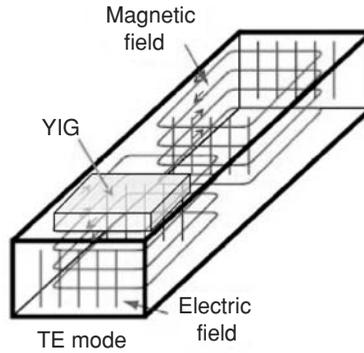
propagation of the electromagnetic waves. Reflecting the microwaves back the
way they came produces double the rotation, not zero rotation.

We briefly describe devices which depend either on resonant absorption of
microwaves, or on the circular birefringence far from resonance which produces
the microwave Faraday effect. Microwave ferrite devices are frequently made
of YIG; highly perfect polished spherical crystals may have a linewidth as low
as $5 \pm 1 \, A \, m^{-1}$ for resonance at 10 GHz. Such a sphere has $Q = f_0/\Delta f \approx 10^5$.
These very sharp resonances are needed for the microwave filters and
oscillators made for communications and measurement systems operating in the
1–100 GHz range.

Microwave devices exploit the difference between μ_+ and μ_- in various
ways. Resonant isolators use the resonance at ω_0 to absorb signals reflected
back along a waveguide, Fig. 12.20. Phase shifters exploit differences between
μ_+ and μ_- above and below the resonance peak. Three- or four-port circulators
transmit signals from one port to the next one, while strongly absorbing on other
paths. Faraday rotators rotate the plane of polarization of the microwaves.

The isolator protects a signal source from reflections of power back down
the waveguide. It operates at resonance, where there is the greatest possible
difference in absorption between the $+$ and $-$ modes. The waveguide transmits
a TE_{01} mode, where the magnetic field is parallel to the broad faces of the guide
and it is circularly polarized in opposite senses in the upper and lower halves
of the waveguide. The pattern of field in the guide is reversed when the wave
travels in the opposite direction. If the top half of the guide is filled with YIG
and a field is applied perpendicular to the broad faces so that its magnetization
precesses in the plane of the H-field, the wave can pass freely in the forward
direction, with attenuation of about 0.3 dB, but it will be strongly alternated, by
up to 40 dB in the reverse direction. The attenuation of the power in the forward
sense is 7%, but in the reverse sense it is 10^4.

A circulator is a device with three or four ports which delivers the input signal
at one port as the output at the next one, while the other ports remain isolated.
The principle of the four-port circulator is illustrated in Fig. 12.21. The heart
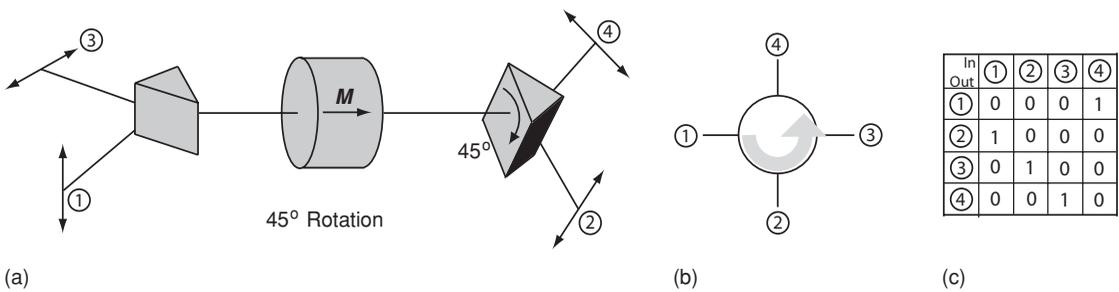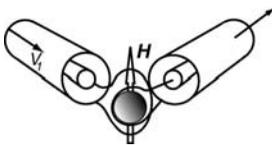
(a)   (b)   (c)

Figure 12.21

A four-port circulator:
(a) illustrates the principle,
(b) shows the sense of
circulation and (c) is the
logic table.

of the device is a YIG disc with thickness and applied field chosen to produce a Faraday rotation of precisely $\pi/4$. The device operates at a frequency where μ_+ and μ_- are sufficiently different to produce the required Faraday rotation, yet far enough from resonance to minimize losses. Two polarization splitters, the microwave equivalent of optical Wollaston prisms, are offset by $\pi/4$ as shown. Each acts to split an incident beam into two perpendicular, linearly-polarized components or conversely to combine them into a single beam. The beam splitting in the microwave device is achieved using single-mode waveguides. A linearly-polarized input at 1 becomes the output at 2. Similarly, an input at 2 becomes an output at 3, and so on. The circulator is a key component of microwave circuits, because it allows a single antenna to be used both for reception and transmission. This was essential for the development of modern telecommunications and radar equipment.

A tunable narrow-band resonant filter is made by winding two orthogonal coils on a small YIG sphere, about 1 mm in diameter. The signal from one coil will only be detected in the other at resonance, where the $+$ mode is circularly polarized. The resonant frequency can be tuned from 1 GHz to more than 10 GHz by changing an externally-applied field.

A resonant microwave
filter. The device transmits
signals in a narrow
frequency range around
the ferromagnetic
resonance frequency f_0.

For higher-frequency, millimetre-wavelength microwave applications such as military phased-array radar, satellite communications or automobile anti-collision radar, the ferromagnetic resonance is not determined by an externally applied magnetic field, but by the anisotropy field of a hard magnet. For $BaFe_{12}O_{19}$, the anisotropy field $\mu_0 H_a = 1.7$ T corresponds to a resonance frequency of 36 GHz when $\mathcal{N} = 1$ (9.17). The resonant frequency can be decreased by scandium substitution or increased by aluminium substitution. These self-biased, miniature high-frequency microwave devices therefore make use of hard magnets, rather than soft magnets.

FURTHER READING

C. W. Chen, *Magnetism and Metallurgy of Soft Magnetic Materials*, New York: Dover Publications (1983). The reprint of this 1977 text provides a wealth of detailed and reliable information on almost every aspect of soft magnets.

R. M. Bozorth, *Ferromagnetism*, Piscataway: Wiley–IEEE Press (1993). The reprint of Bozorth's classic 1951 text remains a reference for metallic materials and electro-magnetic applications.

P. Brissonneau, *Magnétisme et matériaux magnétiques pour l'électrotechnique*, Paris: Editions Hermès (1997). A modern text on low-frequency materials and applications.

P. Beckley, *Electrical Steels for Rotating Machines,* London: IEE (2002). A comprehensive treatment of electrical steels; including information on processing and characterization, with comparisons to other materials.

A. Goldman, *Magnetic Components for Power Electronics*, Dordrecht: Kluwer (2002). A monograph on magnetics for power electronics, covering devices, materials, components and design issues.

J. Nicolas, Microwave ferrites, in *Ferromagnetic Materials* Vol 2, E. P. Wohlfarth (editor), Amsterdam: North Holland (1980).

R. F. Soohoo, *Microwave Magnetics*, New York: Harper and Row (1985).

J. Smit and H. P. J. Wijn, *Ferrites*, New York: Wiley (1979). The standard text on ferrites and their high-frequency applications, by pioneers from Philips.

EXERCISES

12.1 Use the method of dimensions to show that $\delta \propto (\varrho/\mu f)^{1/2}$ and $P_{ed} \propto (if B_{\max}^2)/\varrho$ ((12.2) and (12.4)).

12.2 Deduce the expression for penetration depth (12.2). Estimate how thin a soft metallic film should be if it is to operate at (a) 10 kHz and (b) 1 GHz.

12.3 By considering the field at the apex of a cone of a fully saturated magnetic material produced by the surface magnetic pole density $\mathbf{J} \cdot \mathbf{e}_n$, show that the field is maximum when the half-angle of the cone is $\tan^{-1}\sqrt{2}$.

12.4 Show that the reduction of eddy-current losses in a laminated core scales as $1/N^2$, where N is the number of laminations.

12.5 Estimate (a) the average rate of consumption of electrical energy in watts, per person on Earth, (b) the number of turbogenerators on Earth and (c) the maximum possible diameter of their rotors, if the elastic limit of steel is 700 MN^{-2}.

12.6 Show that the Q-factor for an RL circuit is $L\omega/2R$.